Influence of the synthesis parameters on the properties of natural rubber grafted poly-3-hydroxybutyrate (acte de congrès - 10 pages)

Asmaa Zainal Abidin, Noor Hana Hanif Abu Bakar, Denis Roizard, Anne Jonquieres, Carole Arnal-Herault, Mohamad Abu Bakar, Rosniza Hamzah

INFLUENCE OF VARIOUS SYNTHESIS PARAMETERS ON THE PROPERTIES OF NATURAL RUBBER GRAFTED POLY-3-HYDROXYBUTYRATE

Zainal Abidin, Asmaa[1], Abu Bakar, Noor Hana Hanif[1], Roizard, Denis[2], Jonquieres, Anne[3], Arnal-Herault, Carole[3], Abu Bakar, Mohamad[1] and Hamzah, Rosniza[4]

[1]Nanoscience Research Laboratory, School of Chemical Sciences, Universiti Sains Malaysia, 11800 Penang, Malaysia

[2]Laboratory of Reactions and Process Engineering, Université de Lorraine, UMR CNRS, LRGP, 7274, 1 rue Grandville, 54000 Nancy, France

[3]Laboratoire de Chimie Physique Macromoléculaire, Université de Lorraine, CNRS, LCPM, ENSIC, 1 rue Grandville, BP 20451, F-54 000 Nancy, France

[4]Center of Excellence Geopolymer and Green Technology (CEGeoGTech), Faculty of Engineering Technology (FETech), Universiti Malaysia Perlis (UniMAP), Level 1 Block S2, UniCITI Alam Campus, Sungai Chucuh, Padang Besar, 02100, Perlis, Malaysia

Email: hana_hanif@usm.my

Natural rubber (NR) graft poly-3-hydroxybutyrate (PHB) with a ratio of 60:40 was synthesized in chlorobenzene solvent. Two types of initiators namely azobisisobutyronitrile (AIBN) and benzoyl peroxide (BPO) were utilized to initiate the free radical grafting of the two polymers. The influence of the various types of initiator loadings was also investigated. The position of the PHB grafting on the NR was then determined using ^{1}H, ^{13}C, DEPT 90 and DEPT 145 nuclear magnetic resonance (NMR) analyses and Fourier transformed infrared spectroscopy (FTIR). The thermal stability and crystallization behavior of NR-g-PHB was studied using thermogravimetric analysis (TGA) as well as differential scanning calorimetry (DSC) respectively. The increase in initiator loading improved the grafting. Moreover, single glass transition temperature (T_g) was observed for NR-g-PHB which indicated that no phase separation occurred for the PHB grafts and the thermal stability of the grafted copolymers was improved compared to that of pristine NR and PHB alone.

1.0 Introduction

The development of materials based on renewable resources is currently being considered as one of the most promising ways for overcoming the environmental concerns related to major synthetic polymers. Polymers derived from biomass such as poly(3-hydroxybutyrate) (PHB) have received considerable attention nowadays. PHB is a natural occurring polyester produced by the microorganism, known as *Bacillus megaterium* and was discovered by Lemoigne in 1926 [1]. PHB is a semi-crystalline thermoplastic which is biocompostable, biocompatible as well as renewable in nature [2]. Because of these properties, PHB has been applied in vast applications especially in the biomedical field. PHB not only acts as a vehicle to transport nutrient, drug and bioactive molecule to the tissue or cell, but it is also employed in tissue scaffolding for bone and nerve regeneration, cardiovascular as well as cartilage support respectively [3, 4]. Apart from this, PHB is also used in the field of water treatment. Heitmann and coworkers [5] demonstrated the degradation of methylene blue using PHB as a support to disperse nanostructured niobium oxyhydroxide.

While PHB has shown excellent properties for certain applications, it is a very brittle plastic and prone to thermal degradation at temperatures above the melting point [6]. To a certain extent, this actually limits its application. In an effort to extend its use, various methods have been devised to improve the properties of PHB. Studies have shown that PHB can be blended with other polymers such as ethylene propylene rubber (EPR) [7], poly(methyl methacrylate) (PMMA) [8], polyethylene oxide (PEO) [9] and poly-caprolactone (PCL) [10]. However, as expected, most of the works reported that the polymers did not mix well, and a miscible system rarely occurred. As an example, Graco and Martuscelli [11] studied the blending of PHB with ethylene propylene rubber (EPR). The authors concluded that no interactions occurred between PHB and EPR after two distinct T_g values were observed. Hence, interests in PHB based blends have gradually shifted to reactive systems which allow better mixing and simple preparation method.

Chemical modification of PHB via grafting with NR is an alternative method to incorporate desirable properties without sacrificing its biodegradable nature. NR is a good candidate as it has high elasticity and good rebound resilience [12]. Thus, NR will act as a soft component in the grafted copolymers to achieve better properties or processability which can be employed in biomedical application. A few works have been done on PHB grafting. As an example, Jiang and

Hu [13] investigated the graft polymerization of isoprene onto PHB using radiation technique. A maximum grafting degree of 18% was obtained by varying the solvent, isoprene concentration and irradiation time. Subsequently, Chen et al. [14] employed maleic anhydride (MA) as the grafting monomer to be grafted onto PHB chains. Authors discovered that introducing MA onto PHB chains could disturb the regularity of the PHB chains, control the morphological structures as well as improve its properties. Other works also reported the grafting of PHB onto cellulose via reactive extrusion using dicumyl peroxide as radical initiator [6]. They showed that the thermal stability of PHB was improved after grafting reaction due to the formation of new bonds between PHB and cellulose. Nevertheless, most previous works on PHB grafting used high temperatures around 175 -180 ^{o}C for the grafting reaction [6, 15, 16]. For instance, PHB grafted maleic anhydride was prepared at 175 ^{o}C [15]. According to the authors, as a result of the use of this high temperature, thermal degradation of PHB occurred almost exclusively by random chain-scission. Therefore, in the present study, medium temperature was employed to graft NR with PHB to minimize the occurrence of PHB degradation. This study describes the grafting of NR with PHB in solution using different types of initiators and various parameters that affect the grafting process. Apart from that, several characterization techniques were utilized in this study. The possible structure of the grafted copolymers was further scrutinized using 1D and 2D NMR to confirm the grafting position, since previous literature on NR-g-PHB copolymers did not investigate this in detail [13].

2.0 Materials

Natural rubber latex (NRL, $(C_5H_8)_n$) with 60 % dry rubber content (DRC) was obtained from Malaysian Rubber Board, Kuala Lumpur. Poly(3-hydroxybutyrate) (PHB, 433,000 g/mol) was purchased from BIOCYCLE (Brazil) and purified before use [17]. Chlorobenzene (C_6H_5Cl, 99.7 %) and acetone (C_3H_6O) were purchased from Sigma Aldrich (USA). Azobisisobutyronitrile (AIBN, $C_8H_{12}N_4$) and benzoyl peroxide (BPO, $C_{14}H_{10}O_4$) were manufactured by Fluka (UK). Besides that, deuterated chloroform (99.8%, $CDCl_3$) for NMR analysis was purchased from Merck (USA) and argon (99% purity) gas was purchased from Linde (Malaysia).

2.1 Preparation of dry rubber (DR)

DR was obtained by coagulation of NRL in a glass bottle containing acetone at room temperature. The acetone was removed after coagulation and the coagulates were washed again using acetone several times. Finally, the coagulates were dried in a vacuum oven at 40 °C until constant weight was reached.

2.2 Preparation of NR-g- poly (3-hydroxybutyrate) copolymers

DR and PHB with a 60:40 wt/wt ratio were dissolved in chlorobenzene at 105 °C overnight. The initiator, AIBN, was added into the cooled polymer mixture at 30 °C followed by 15 min stirring. The polymer mixture was cast in a glass mold, purged with argon gas, and covered with a glass plate. Afterwards, the NR-g-PHB was kept in the oven for 2 days at a certain casting temperature to maximize the grafting and cross-linking reactions. The glass plate cover was then removed to achieve solvent evaporation at casting temperature. Different casting temperatures and initiator loadings were investigated as in Table 1. These steps were repeated with another initiator (BPO) allowing working at slightly higher temperature.

Table 1: Parameters for the study of NR-g-PHB synthesis.

NR-g-PHB	Type of initiator	Casting Temperature (^{o}C)	Initiator loading (% mol)
60:40	AIBN	90	7
	BPO	90	7
60:40	BPO	105	3
	BPO	105	5
	BPO	105	7
	BPO	105	10

2.3 Characterization

The structural characterization of the grafting reaction was carried out by using NMR spectroscopy. The spectra were obtained using *Bruker BioSpin ADVANCE* at 500 MHz and 300 MHz for ^{1}H NMR and ^{13}C NMR, respectively. Complementary DEPT 90 and DEPT 135 analyses

were performed at 25 ^{o}C in a flow of air. The samples were dissolved in deuterated chloroform ($CDCl_3$) and tetramethylsilane (TMS) was used as an internal standard. In addition, the possible structural changes of the samples were confirmed by Fourier Transformed Infrared (FTIR) spectroscopy. The samples were scanned from 400-4000 cm^{-1} using a *Frontier Universal ATR Perkin Elmer FT-NIR Spectrometer*. The thermal properties of the samples were studied using a *Mettler Toledo Differential Scanning Calorimetry*. As much as 10 mg of the samples were weighed in an aluminum pan and covered with an aluminum lid. The sample was heated from -100 to 190 ^{o}C and held for 2 min at a heating rate of 20 ^{o}C min^{-1} under nitrogen environment. Next, the samples were quenched to -100 ^{o}C at a scanning rate of 20 ^{o}C min^{-1} and held for another 2 min. Finally, the samples were again heated to 190 ^{o}C at a heating rate of 20 ^{o}C min^{-1}. Meanwhile, 5.00 mg of the samples were heated from 30 ^{o}C to 900 ^{o}C at a heating rate of 20 ^{o}C min^{-1} under nitrogen flow to examine thermal stability using *Perkin Elmer STA 6000* simultaneous thermal analyzer.

3.0 Results and discussion

3.1 Effect of initiator

Two initiators, AIBN and BPO were studied using the same initiator concentration of 7 % mol at 90 ^{o}C to investigate their effectiveness in grafting NR with PHB. When AIBN initiator was employed, the NR-g-PHB copolymer formed a lot of small separated pieces on the glass mold as compared to the BPO initiator, which gave a smoother surface as shown in Figure 1 (a-b). The breakages in the NR-g-PHB membrane could be due to the insufficient occurrence of grafting and/or crosslinking between NR and PHB, which can be proven by the rapid dissolution of the grafted polymer in chloroform solvent. AIBN is known as a good thermal initiator for moderate temperatures (e.g. 60°C). At 90°C, it was not an effective initiator mainly because at this higher temperature, its decomposition rate was too high. Therefore, an initiator (BPO) with a moderate decomposition rate at the grafting temperature was then chosen to ensure that the initiating phenyl radicals would be produced during the whole grafting process. BPO contains a weak sigma bond (O-O bond), which could rapidly undergo bond homolysis at the grafting temperature to generate a pair of radicals, which were then fragmentated to provide phenyl radicals as depicted in Figure 2 (b). These phenyl radicals are capable in abstracting a hydrogen atom from a carbon-hydrogen bond in either NR or PHB [19]. In addition, BPO could also be used at temperatures 90-110 ^{o}C due to the fact that its half-life in chlorobenzene is much longer in comparison to AIBN. In this

work, the choice of the grafting temperature range (90-105 °C) resulted from a compromise. It had to be high enough for improving NR grafting and, at the same time, it had to be limited for avoiding PHB degradation. Therefore, it would provide advantages compared to previous works reporting grafting and crosslinking for NR usually at much higher temperatures (170-180 ºC) [20]. Hence, for the next part of this study, BPO was selected as the initiator in the preparation of NR-g-PHB copolymers in the temperature range 90-105 °C.

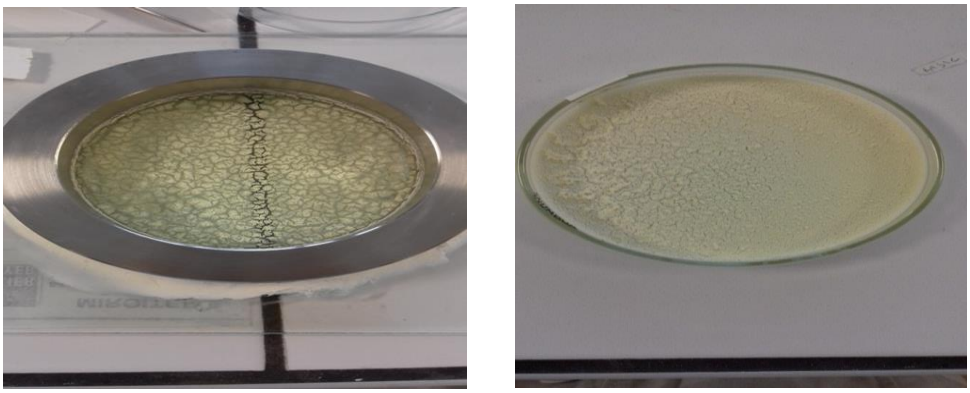

(a) (b)

Figure 1: Images of membranes obtained for different initiator (a) AIBN and (b) BPO using 7 % mol at 90 ºC.

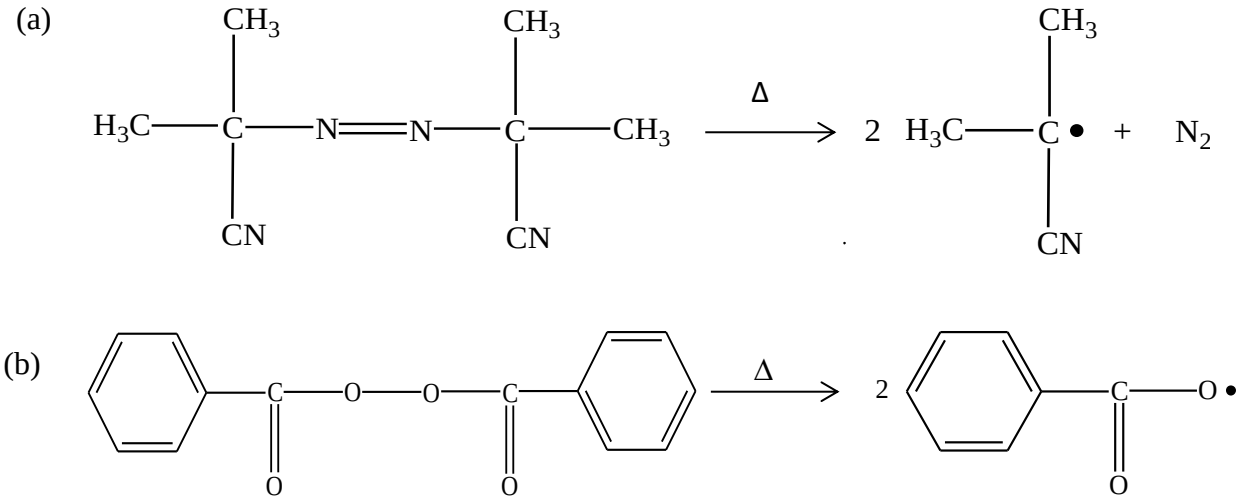

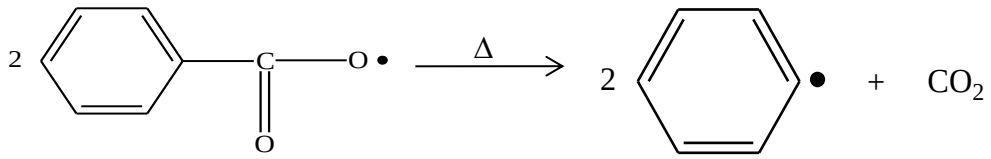

Figure 2: Radical formation from (a) AIBN and (b) BPO.

The effect of initiator loadings on the preparation of NR-g-PHB was investigated and the membrane images are illustrated in Figure 3. The experiments were performed using various BPO initiator concentrations ranging from 3 to 10 % mol. The same weight ratio 60:40 for NR and PHB was used for the synthesis of the NR-g-PHB copolymers with reaction temperature of 105 °C. When the initiator loading was increased, the membrane breakage was greatly reduced. For the highest initiator loadings, homogeneous membranes were obtained. This improvement can be explained as due to the increasing amounts of free radicals that were produced from the dissociation of BPO, resulting in more active sites on the NR and PHB backbones, thus facilitating grafting. However, for the maximum initiator loading of 10 % mol., the membrane retracted from the mold border (Fig 3d). Therefore, from these results, the optimum BPO amount was taken to be 7 % mol (Fig 3c).

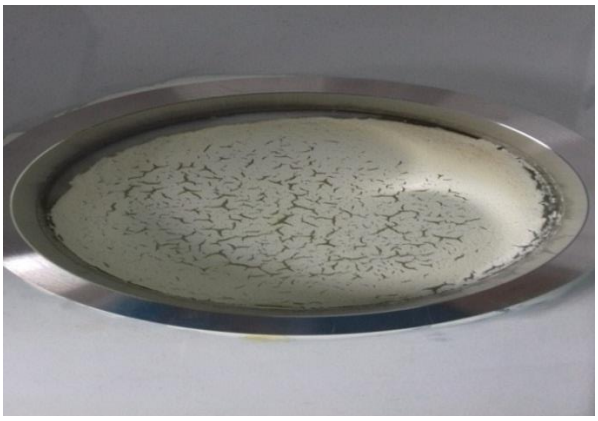

(a)

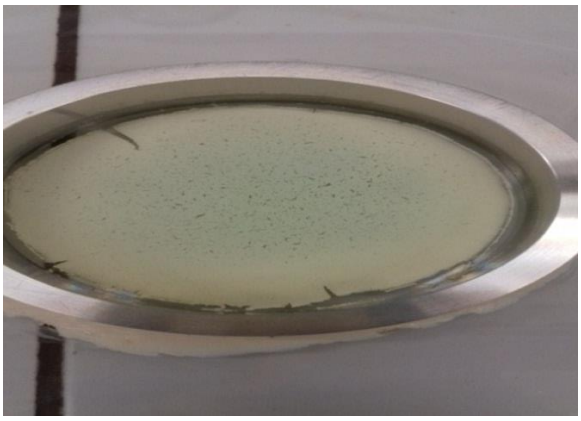

(b)

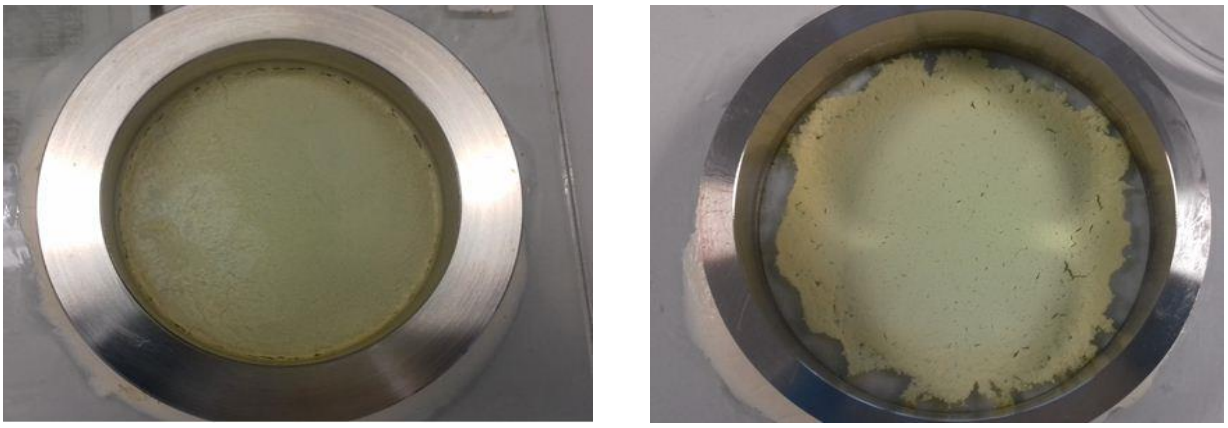

(c) (d)

Figure 3: Images of NR-g-PHB membranes obtained for (a) 3, (b) 5, (c) 7 and (d) 10 % mol of BPO loadings at 105 °C.

3.2 Characterization of NR-g-PHB copolymers

3.2.1 NMR Spectroscopy

The confirmation of the chemical structure of the pristine NR, PHB and NR-g-PHB was further obtained using ^{1}H and ^{13}C NMR spectrum as presented in Figures 4, 5 and 6, respectively. In this work, the NR, PHB and NR-g-PHB structures were labeled to identify the carbon position and its respective proton(s). For facilitating the assignments of the different peaks for the grafted copolymers, labelling by numbering was chosen for the main chain (NR) and labelling by lettering was selected for the grafts (PHB). For the ^{1}H NMR spectrum of NR in Figure 4 (a), the unsaturated methyne proton 3 of the double bonds, the methyl protons 5 and allylic methylene protons 1 and 4 resonated at δ_H 5.04-5.06 ppm, δ_H 1.61 ppm and δ_H 1.97 ppm, respectively. On the other hand, five ^{13}C NMR signals of NR resonated at δ_C 23.42 ppm, δ_C 26.40 ppm, δ_C 29.90 ppm, δ_C 125.04 ppm as well as δ_C 135.21 ppm as observed in Figure 4 (b). These carbon signals are attributed to the methyl carbon 5, allylic methylene carbons 4 and 1, methyne carbon 3 and the other carbon of the double bonds corresponding to carbon 2. These chemical shifts in the ^{1}H and ^{13}C NMR of NR were in good agreement with previous works [21-26].

(a)

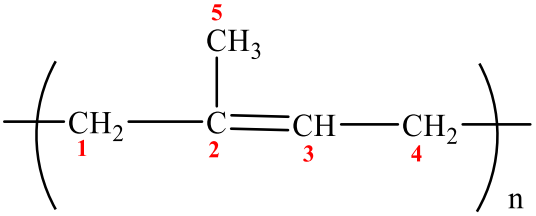

(NR)

^{1}H chemical shifts of NR (ppm)

5 (δ_H 1.61)
1 and 4 (δ_H 1.97)
3 (δ_H 5.04-5.06)

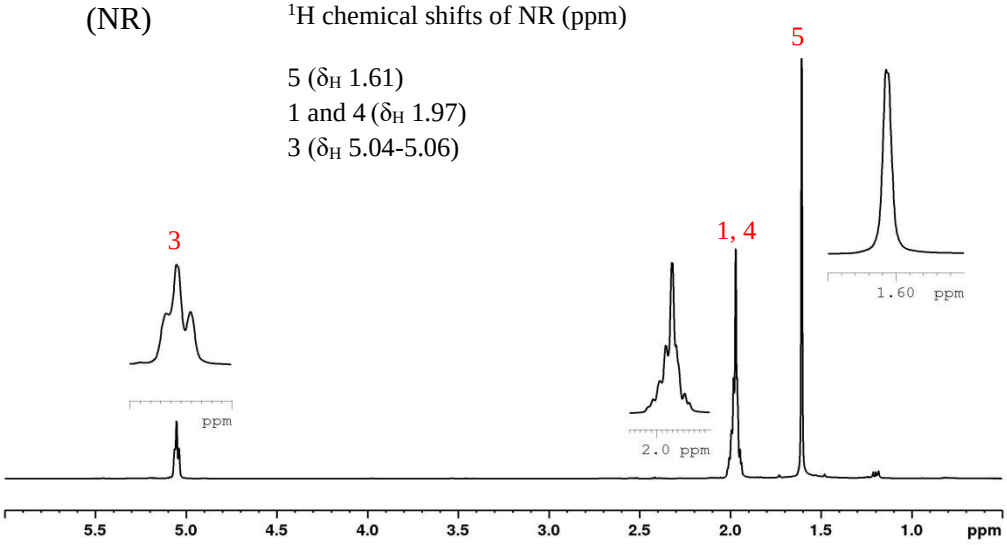

(b)

^{13}C chemical shifts of NR (ppm)

5 (δ_C 23.42)
4 (δ_C 26.40)
1 (δ_C 29.90)
3 (δ_C 125.04)
2 (δ_C 135.21)

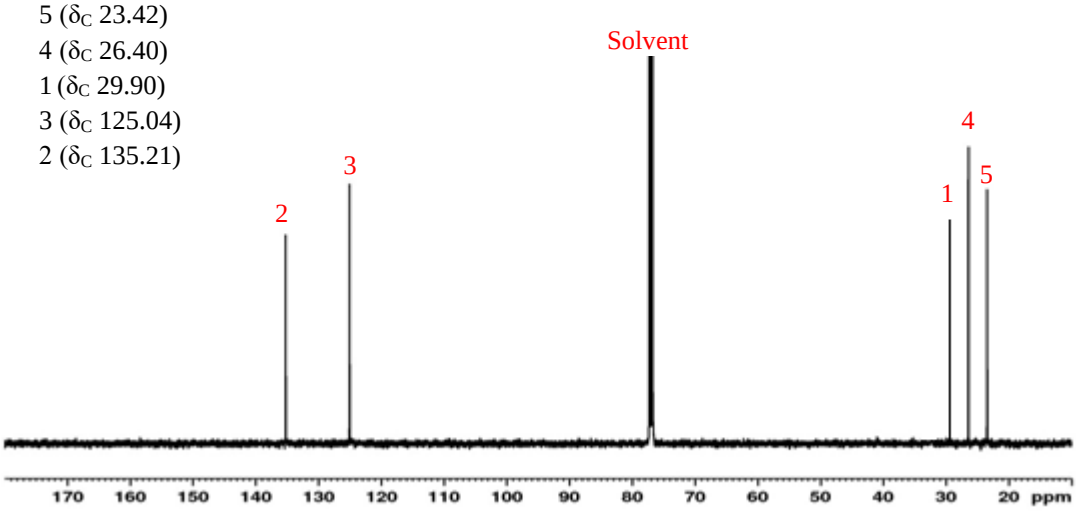

Figure 4: NMR spectrum for (a) ^{1}H and (b) ^{13}C of NR.

As can be seen in Figure 5 (a), the ^{1}H NMR spectrum of PHB showed a doublet at the δ_H 1.20-1.21 ppm which is attributed to the methyl protons D. These protons were highly shielded and absorbed at the most upfield region. Besides that, the methylene protons B showed a mirror quartet signal that resonated in the range of δ_H 2.38-2.56 ppm. Meanwhile and as expected, the multiplet signal in the range δ_H 5.17-5.21 ppm corresponded to the methyne proton A. This signal resonated at the most downfield region because these methyne protons were deshielded by an electronegative oxygen atom due to inductive effect of the ester group. In Figure 5 (b), PHB exhibited four carbon peaks at δ_C 19.76 ppm, δ_C 40.81 ppm, δ_C 67.62 ppm and δ_C 169.12 ppm that were assigned to methyl carbon D, methylene carbon B, methyne carbon A and carbon C of the carbonyl of the ester group, respectively. These NMR spectra confirmed the purity of PHB, and the assignments of the different peaks were consistent with previous works [27-32].

(a)

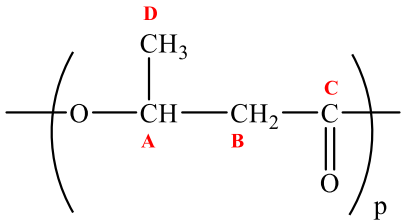

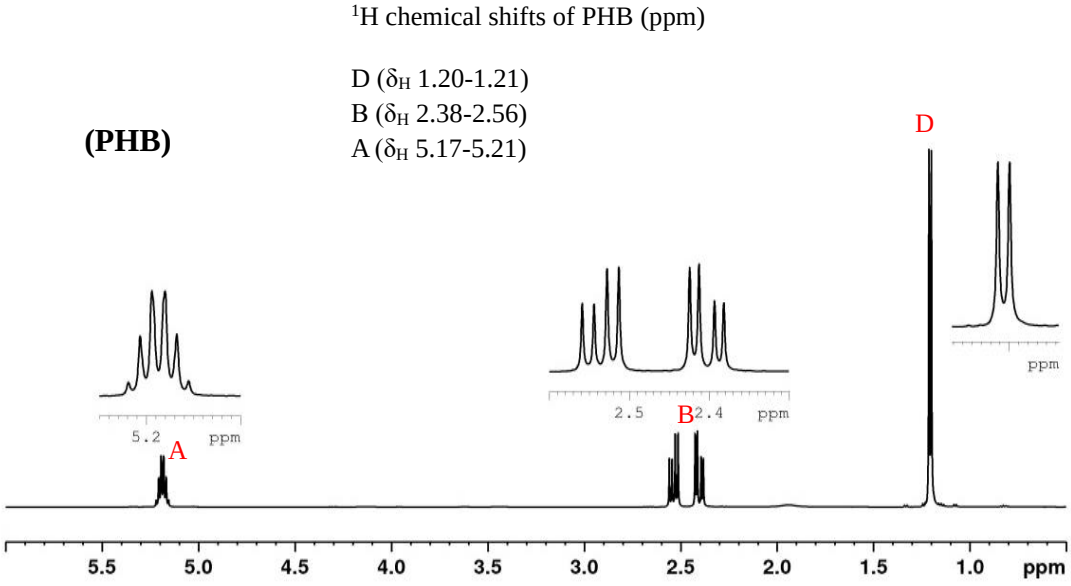

(b)

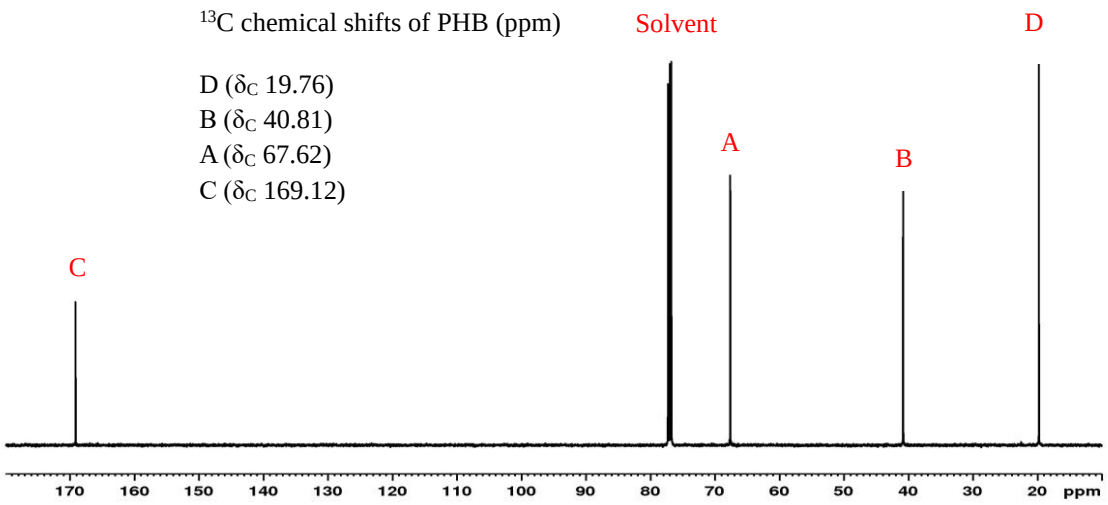

Figure 5: NMR spectrum for (a) ^{1}H and (b) ^{13}C of PHB.

The grafting of PHB onto NR in the presence of BPO at high temperature can proceed in two different ways (Figure 6). In type I grafting, an allylic H is abstracted from the NR chain by the phenyl radical resulting from BPO decomposition, followed by coupling of the resulting allylic radical with a PHB chain bearing a radical. The formation of such allylic radical is very easy because this allylic radical is strongly stabilized by resonance involving the adjacent double bond. In this first type of grafting, the NR double bonds remain unchanged. In type II grafting, first, there is an addition of the phenyl radical onto the NR double bond. Then, the corresponding radical is coupled with a PHB chain bearing a radical. The formation of a radical onto PHB mainly occurs through H abstraction by the phenyl radical. The most favored site for this abstraction is on the ternary carbon atom to generate a stabilized tertiary radical. After coupling, this ternary carbon atom becomes a quaternary carbon, which does not bear any hydrogen atom.

(a)

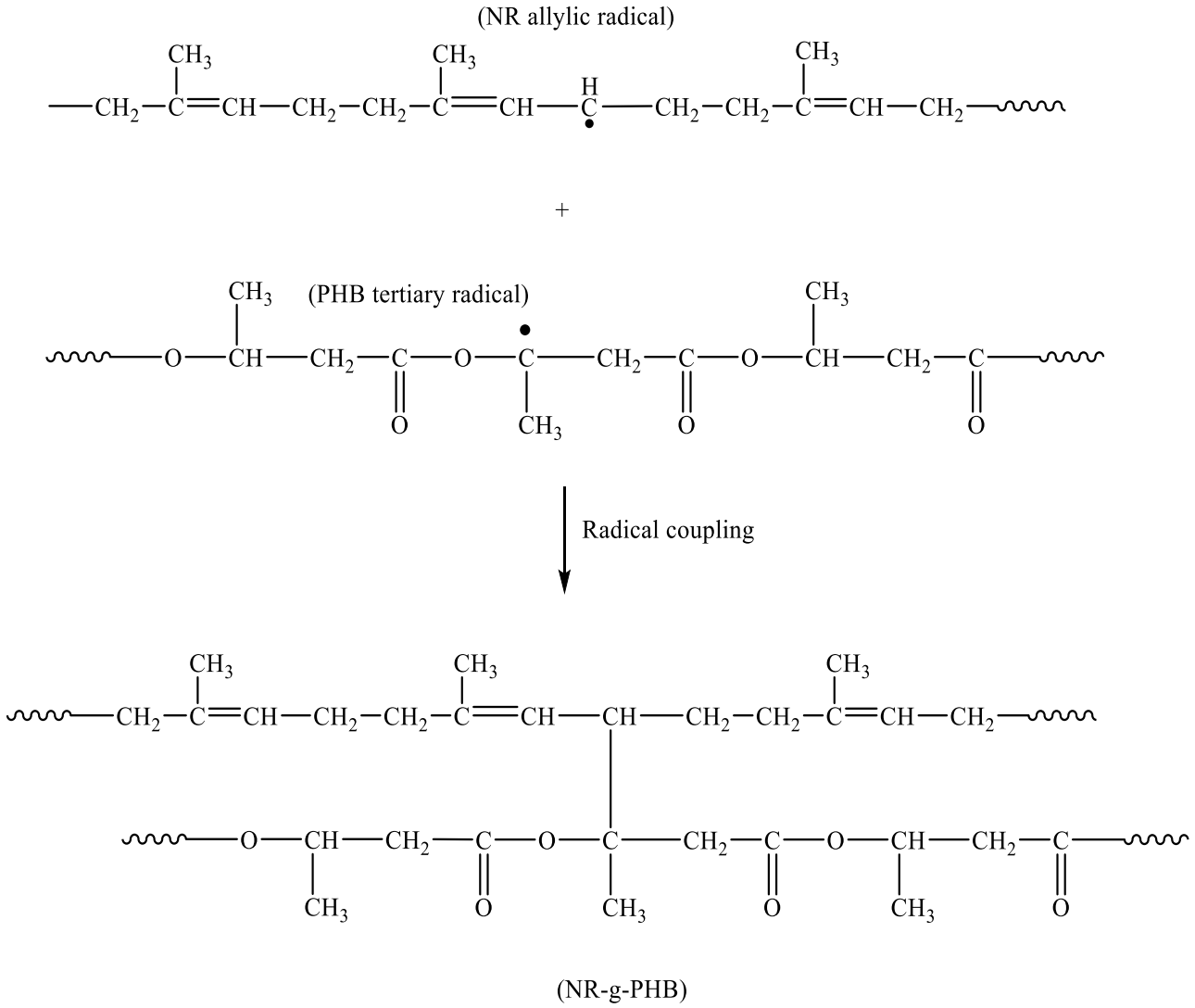

(NR-g-PHB)

(b)

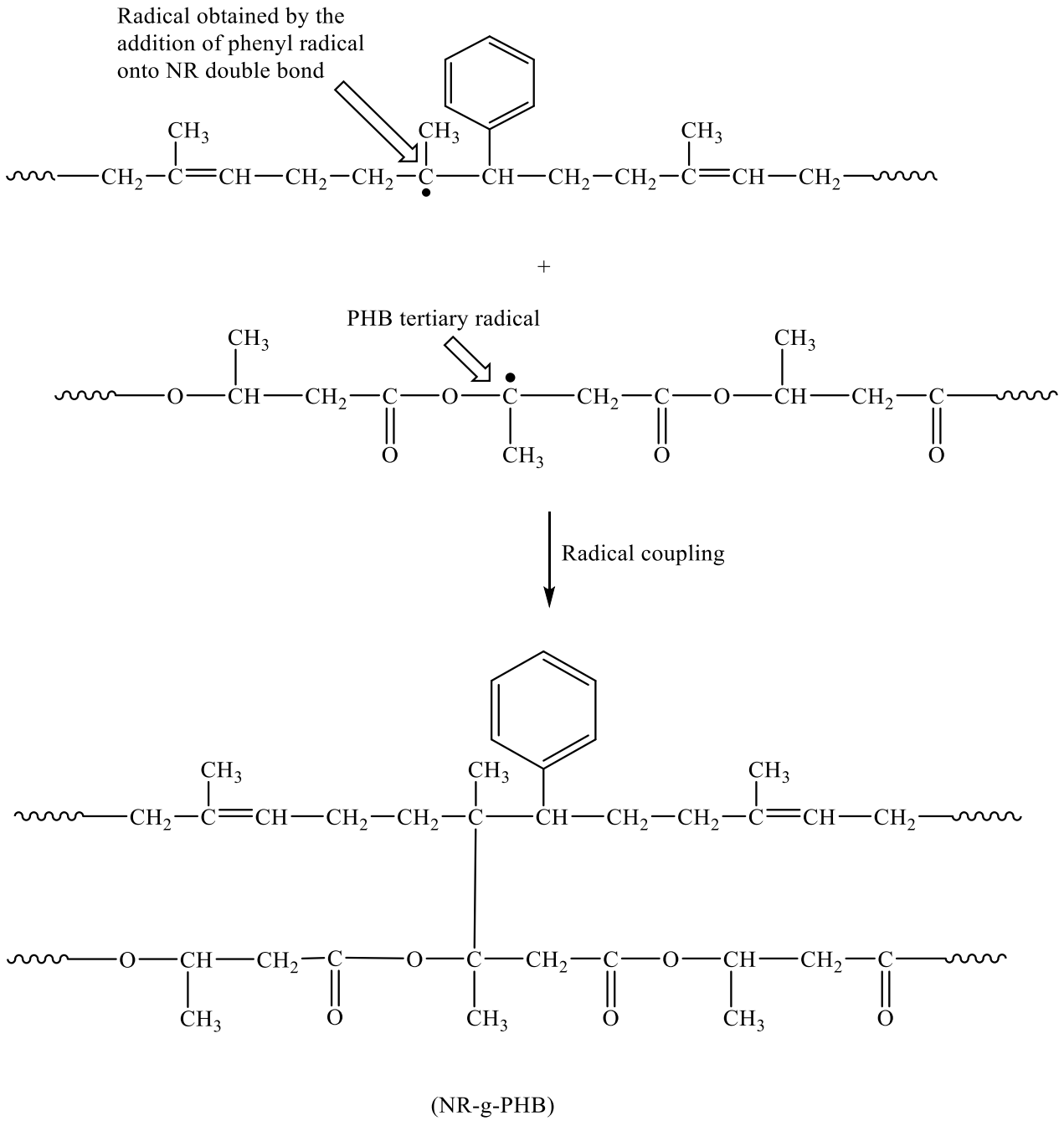

(NR-g-PHB)

Figure 6: Mechanisms for PHB grafting onto NR. (a) Type I grafting, an allylic H abstraction followed by radical coupling and (b) Type II grafting, an addition of phenyl radical onto NR double bond followed by radical coupling.

As illustrated in Figure 7 (a) and (b), ^{1}H and ^{13}C NMR spectra of NR-g-PHB showed all the signals for the NR and PHB ungrafted monomer units because of the low grafting rate. In particular, the methyne protons of the NR double bonds are responsible for a peak at δ_H 5.04-5.05 ppm in the ^{1}H NMR spectrum (Fig 7 (a)). These double bonds were still numerous after grafting, because it only disappears by type II grafting after the addition of phenyl radical to the double bonds. Meanwhile, in type I grafting, the double bonds remained in the corresponding grafted monomer units after the allylic H abstraction. These double bonds were also responsible for two peaks in the ^{13}C NMR spectrum at δ_C 124.2 ppm (carbons 3) and δ_C 134.5 ppm (carbons 2) (Fig 7 (b)).

As expected from the low grafting rate, new NMR signals related to the grafted monomer units were scarce and of weak intensity. The broad tiny peak in the range of δ_H 7.33-7.42 ppm in the ^{1}H NMR spectrum was characteristic for the proton of the phenyl rings attached the NR chains after type II grafting. The very weak intensity of this broad peak shows that type II grafting was minor. In the ^{13}C NMR spectrum, as expected, the new corresponding peaks were hardly detectable at δ_C 127.12-128.42 ppm due to the much lower ^{13}C abundance.

The new methyne protons related to the grafting sites were not detected in the ^{1}H NMR spectrum, most likely because this peak was overlapped by other peaks (1,4). However, in the ^{13}C NMR spectrum, two tiny new peaks were characteristic for these grafted sites. The first one at δ_C 31.19 ppm corresponded to the carbons 4' of the methyne group attached to PHB during type I grafting. This assignment is in good agreement with the chemical shift calculated by ChemDraw Ultra simulation (δ_C 32.8 ppm) for this methyne carbon. It is important to note that the chemical shift (δ_C 40 ppm) calculated for the methyne carbon 3" resulting from type II grafting occurs at a significantly higher chemical shift due to the attached phenyl ring. The intensity of the peak related to this methyne carbon 3" was too low to be detected in the ^{13}C NMR spectrum, as expected from the hardly detectable phenyl carbons attached to the NR chains during type II grafting.

The other new peak at δ_C 71.90 ppm corresponded to the quaternary carbon A' of the grafted PHB monomer units. As expected, the intensity of this new peak related to carbon A' is much lower than that of the peak for the related carbon 4', because carbon A' are quaternary carbon not bearing any hydrogen atom. Here again, the quaternary carbon A" resulting from type II grafting, which would appear at a slightly higher chemical shift, were too scarce to be detected on

the ^{13}C NMR spectrum. Therefore, the ^{1}H and ^{13}C NMR spectra of the grafted copolymer both show that type I grafting prevailed and that the grafting rate was low, as expected because all the grafted copolymers remained soluble in chloroform.

(a)

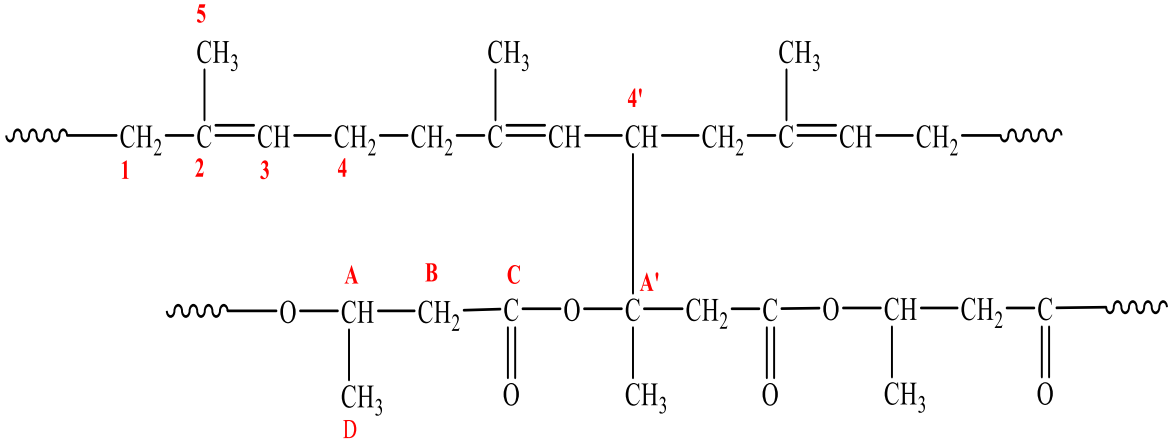

(Type I NR-g-PHB)

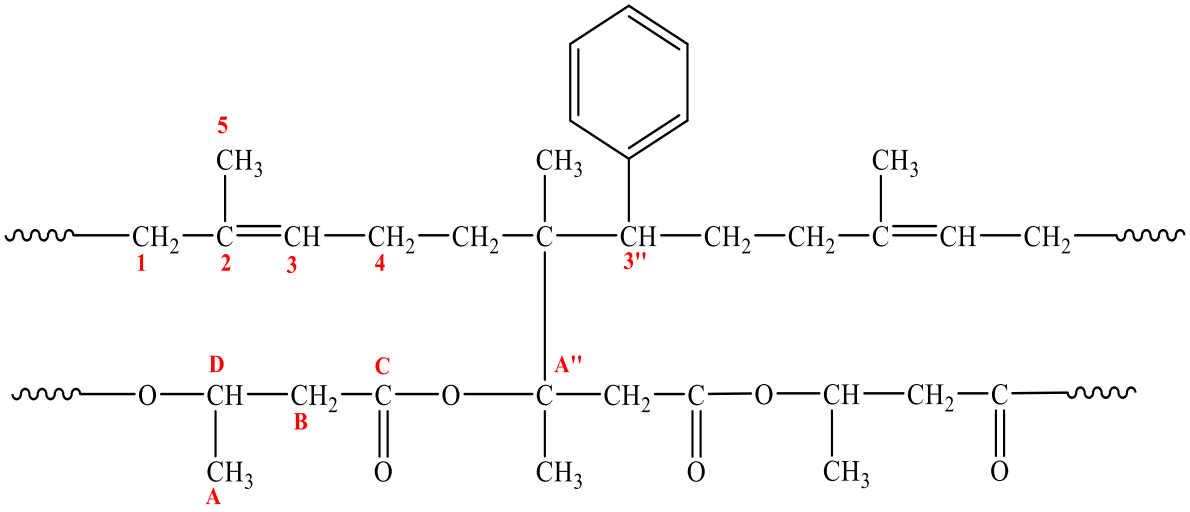

(Type II NR-g-PHB)

^{1}H chemical shifts of NR-g-PHB (ppm)

Related to NR monomer units:
5 (δ_H 1.61), 1,4 (δ_H 1.97)
3 (δ_H 5.04-5.05)
Related to PHB monomer units:
D (δ_H 1.20-1.21) B (δ_H 2.38-2.56)
A (δ_H 5.16-5.22)
New peaks after grafting:
Phenyl (δ_H 7.33-7.42)

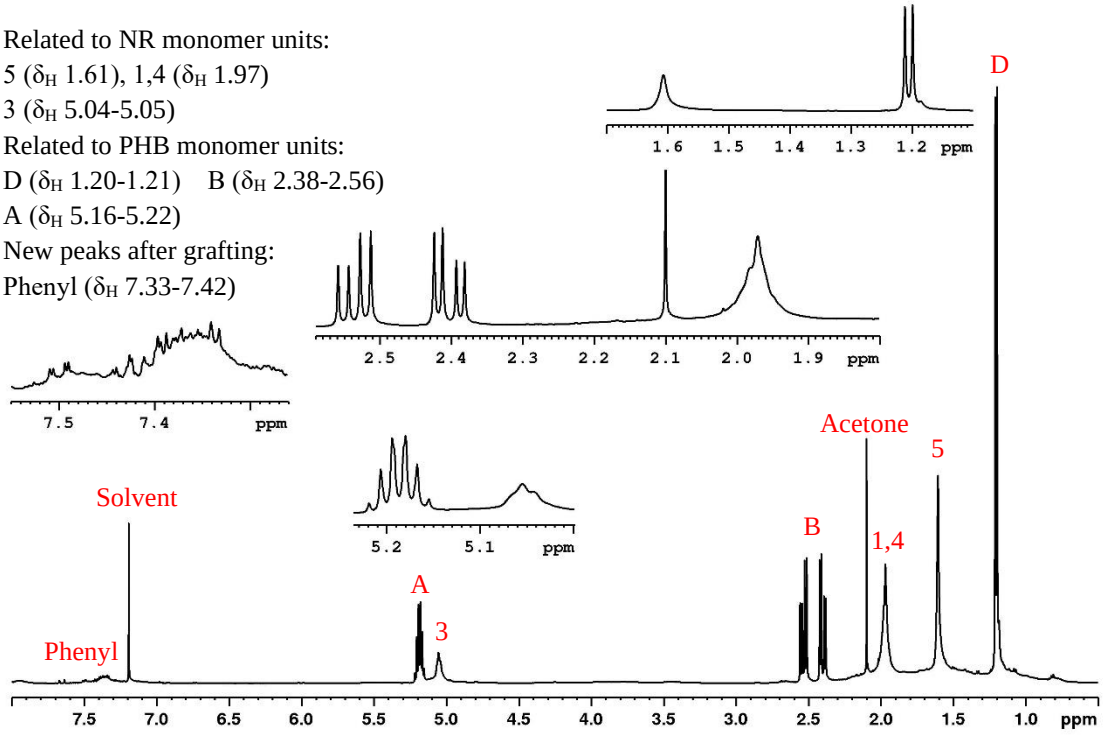

(b)

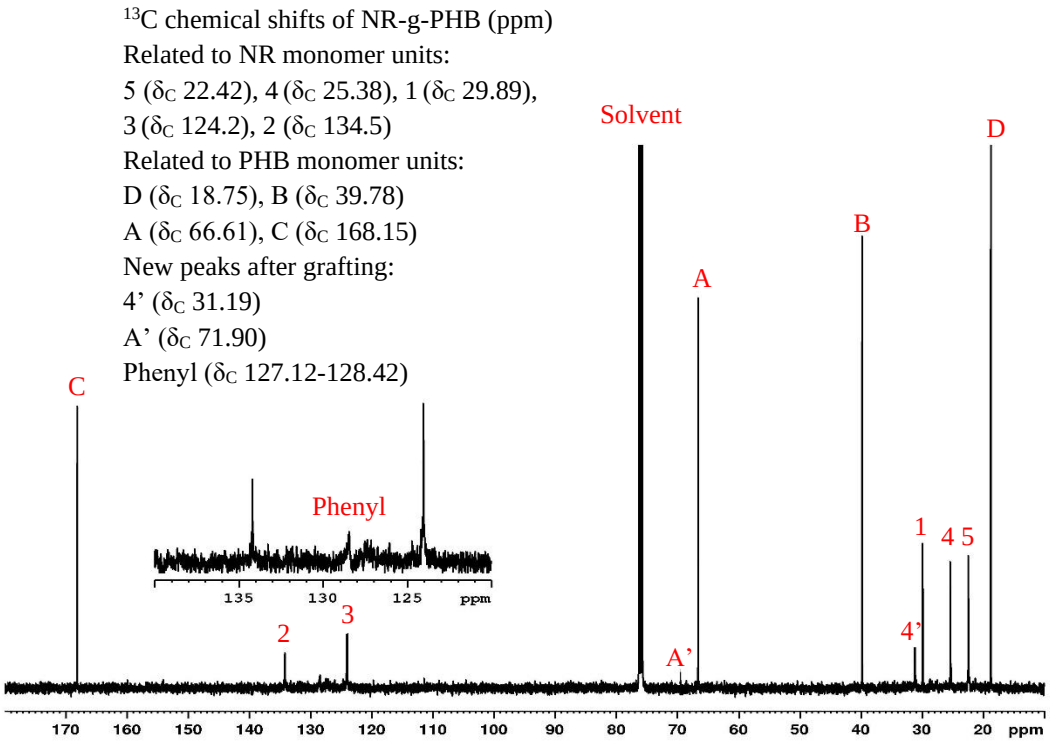

Figure7: Enlarged NMR spectrum for (a) ^{1}H and (b) ^{13}C of NR-g-PHB.

To further confirm assignment of the new peaks resulting from grafting, all carbon signals were characterized using DEPT 90 and 135 experiments. As shown in Figure 8 (a), four methyne signals were observed in the DEPT 90. These signals resonated at δ_C 66.61 ppm, δ_C 31.19 ppm, δ_C 124.2 ppm and δ_C 127.12-128.42 ppm, which were assigned to the methyne carbon A, 4', 3 and phenyl rings attached to the NR main chain after type I and II grafting, respectively. The assignment of the new peak related to the methyne carbon 4' obtained after type I grafting was thus confirmed by the DEPT 90 analysis. In contrast, three peaks for the methylene carbon (4, 1 and B) of NR-g-PHB showed negative signals in the DEPT 135 spectrum shown in Figure 8 (b). Meanwhile, in the positive region, the two methyl carbon signals (D and 5) of PHB and NR resonated at δ_C 18.75 ppm and δ_C 22.42 ppm. As expected, similar methyne carbon signals as in the DEPT 90 also appeared in the positive region of DEPT 135. As can be seen here, a new signal at δ_C 71.90 ppm corresponding to carbons A' did not appear in the DEPT 90 and 135, which proves

that this signal corresponded to quaternary carbon atoms not bearing any hydrogen atom in good agreement with the proposed structure in Figure 6.

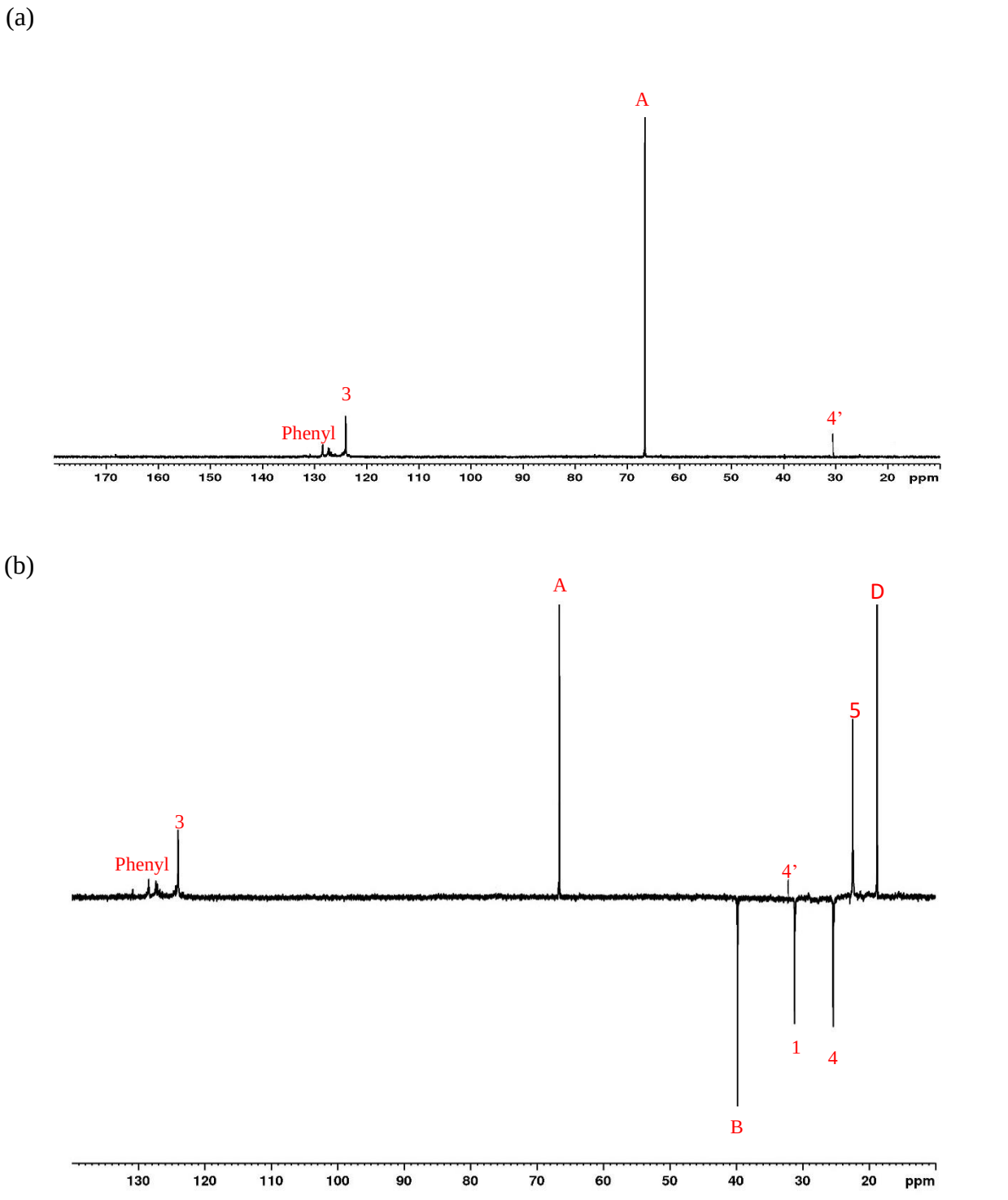

Figure 8: DEPT (a) 90 and (b) 135 spectrum of NR-g-PHB.

3.2.2 FTIR Spectroscopy

Figure 12 show the FTIR spectra of pristine NR and PHB. PHB showed several peaks as presented in Figure 12 (a). The most important characteristic peak in the PHB spectra is the carbonyl stretching vibration (C=O) which occurred at 1720 cm^{-1}. The peak at 1099 cm^{-1} corresponded to C-O-C stretching vibration and the peaks at 2932 and 2974 cm^{-1} are assigned to sp^3 –CH bond respectively. In addition, the various modes of CH_3 deformation give rise to peaks at 1453 cm^{-1} (asymmetric deformation) and 1379 cm^{-1} (symmetric deformation). All the data here closely resembled data obtained by previous studies [30, 35]. In addition, Figure 12 (b) showed the FTIR spectrum of NR. The NR spectrum confirmed the presence of the C=C bond at 1661 cm^{-1} (stretching vibration of medium intensity) and (=C-H) out-of-plane bending which causes the peak at 833 cm^{-1}. Other peaks occur at 2961 cm^{-1} which refers to the asymmetric vibration of CH_3, at 2920 cm^{-1} which is attributed to the asymmetric vibration of CH_2 and at 2852 cm^{-1} which corresponds to the symmetric vibrations of CH_3 and CH_2. On the other hand, the peaks at 1375 cm^{-1} and 1446 cm^{-1} represents the CH in-plane deformation related to the NR double bond and CH_2 bending, respectively.

Subsequently, Figure 12 (c) showed a typical NR-g-PHB spectrum prepared using 7 % mol of BPO. As can be seen here, both characteristic peaks of PHB and NR were observed in the NR-g-PHB spectra. As an example, the peak for asymmetric vibration of -CH_3 of NR was found at 2869 cm^{-1}, meanwhile the peak for C=O of PHB was observed at 1720 cm^{-1}. However, the peak at 1661 cm^{-1} related to the stretching vibration of the NR double bonds did not clearly appear in the NR-g-PHB spectrum. However, from the NMR data, it was obvious that these double bonds were still present in the grafted copolymer and this weak FTIR peak overlapped with the strong C=O peak of PHB as illustrated in Figure 12 (c). Interestingly, the peak at 827 cm^{-1} characteristic for the (=C-H) out-of-plane bending related to the NR double bonds was still clearly observed in the spectrum of the grafted copolymer. Its reduced intensity compared to that of pure NR was related to presence of 40 wt% of PHB in the grafted copolymer and also to the reaction of some of the NR double bonds during NR grafting. These findings corroborate with the NMR results from the previous section.

Furthermore, the change in the crystalline phase of PHB could further support that modification occurred. As can be seen in Figure 12 (a), three prominent peaks attributed to the

crystallinity of PHB occurred at 980 cm^{-1}, 1230 cm^{-1} as well as 1720 cm^{-1} [6]. Noticeably, the peak intensity attributed to crystalline PHB at 980 cm^{-1} and 1230 cm^{-1} for NR-g-PHB was reduced when compared to PHB alone. In addition, an intense and broad shoulder at 1720 cm^{-1} attributed to the amorphous region of PHB was observed in Figure 13. The entanglement of the grafted NR might have obstructed the lamellar structure of the crystalline phase of PHB, resulting in a more amorphous PHB. Wei et al. [6], discovered a similar observation when grafting PHB onto cellulose causing a reduction in the intensity of the crystalline peak and a broad shoulder attributed to amorphous PHB. Thus, it could be deduced from FTIR results, that NR had successfully modified PHB.

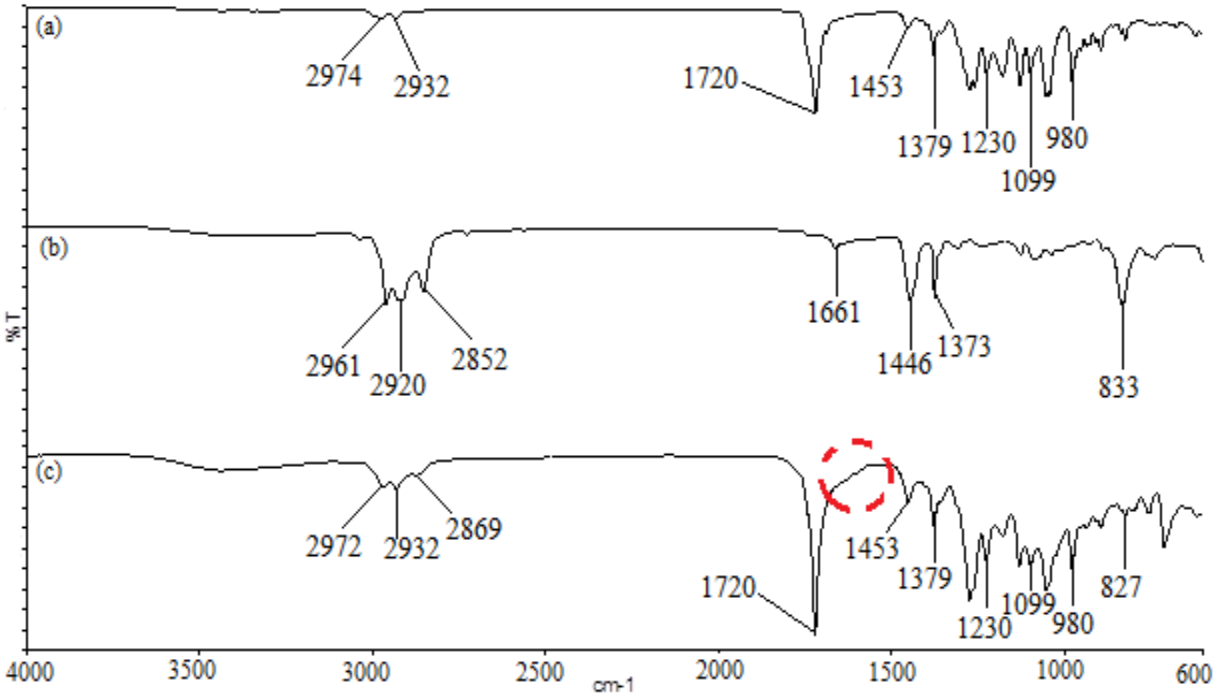

Figure 12: FTIR spectra of (a) pristine PHB, (b) NR and (c) typical of 7 % mol of BPO initiator on NR grafting by PHB at 105 ^{o}C.

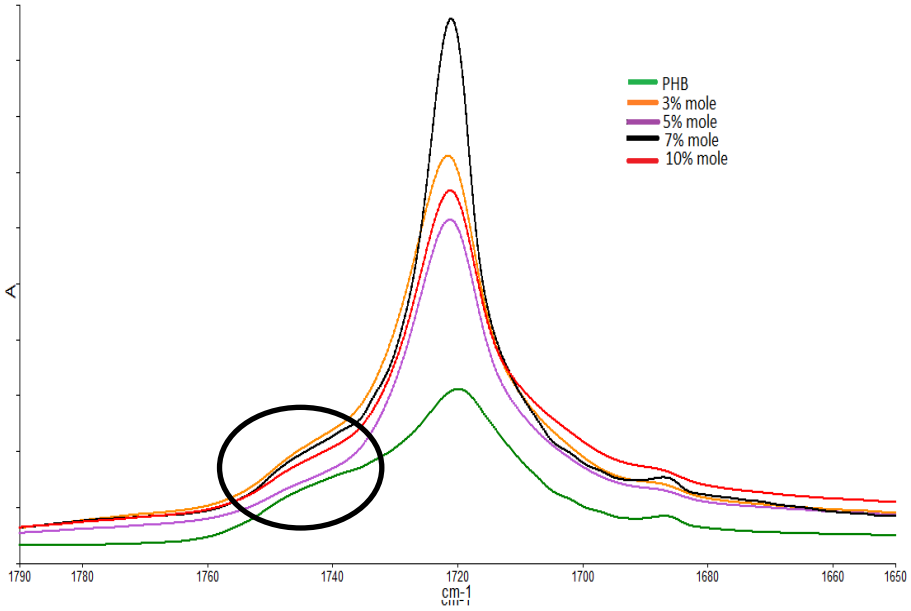

Figure 13: Expanded region of FTIR spectra for PHB and NR-g-PHB with various initiator loading.

3.4 Thermogravimetry Analysis (TG-DTG)

TG and DTG thermograms of pristine NR, PHB and NR-g-PHB prepared using different % mol of BPO initiator are presented in Figure 14 (a) and (b). The T_{onset} values as well as maximum degradation temperature (T_{max}) are summarized in Table 2. As can be seen, NR and PHB exhibited a single stage thermal degradation profile, meanwhile a three stage thermal degradation profile was found for NR-g-PHB prepared using 3, 5 and 10 % mol of BPO. However, a two stage thermal degradation profile was observed when 7 % mol BPO was used. NR and PHB showed that the T_{onset1} occurred at 363 ^{o}C and 286 ^{o}C with T_{max1} values at 380 ^{o}C and 292 ^{o}C respectively.

Meanwhile, for the NR-g-PHB, the first stage of degradation temperature (T_{onset1}) occurred at around 155-198 ^{o}C with T_{max1} at 209-232 ^{o}C. This stage is attributed to the short chain length of PHB which is produced from the chain scission reaction. This finding was similar to Lee and coworkers [17]. They discovered that the melt reaction of PHB/ENR starts with a random thermal scission of long chain PHB molecules to shorter chains bearing carboxyl ends. The second degradation stage which has a T_{onset2} at 272-285 ^{o}C and T_{max2} of 297-312 ^{o}C was attributed to the grafted portion of PHB chains. The value of T_{onset2} for the NR-g-PHB prepared using 3, 5, 7 and 10 % mol of BPO was slightly lower when compared to T_{onset1} of neat PHB. This phenomenon is

due to the heat transfer effect from the shorter PHB chains (first stage) which triggered the T_{onset} at the second stage to occur earlier. Finally, the last stage has a T_{onset3} in the temperature range of 363-380 ^{o}C with a T_{max3} between 412-427 ^{o}C. This degradation stage can be attributed to cross-linked and grafted NR. The T_{max3} values of this stage is higher than pristine NR and PHB as shown clearly in the derivative thermogravimetric graph. This indicated that the NR-g-PHB had improved thermal stability compared to pristine NR and PHB. Furthermore, the amount of char residue of NR and PHB was not found whilst it was about 1-5 % residual for the NR-g-PHB. In addition, grafting with 7 % mol of initiator showed a large residual at around 5.13 %. This result demonstrated the ability of NR-g-PHB to resist heat higher when compared to NR and PHB alone.

(a)

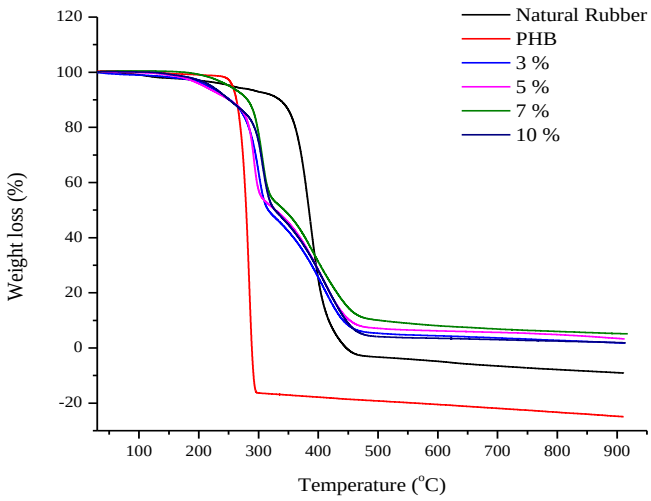

(b)

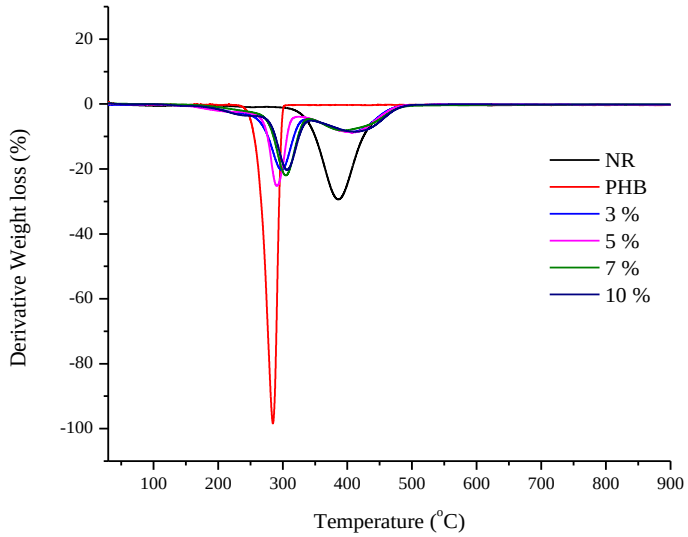

Figure 14: (a) TG and (b) DTG curves obtained for (a) NR and PHB as well as (b) NR-g-PHB prepared using different mol % of BPO.

Table 2: Thermal data of pristine NR, PHB and NR-g-PHB with different loading of BPO initiator.

Different loading of BPO	T_{onset} (TG curve)			T_{max} (DTG curve)			Final Residual
	T_1	T_2	T_3	T_{max1}	T_{max2}	T_{max3}	
NR	363	-	-	380	-	-	0
PHB	286	-	-	292	-	-	0
3	195	272	371	209	297	425	1.76
5	198	279	364	215	290	425	3.28
7	-	283	363	-	310	412	5.13
10	155	285	380	232	312	427	1.88

3.5 Differential Scanning Calorimetry (DSC)

Figure 15 (a) and (b) showed the DSC heating curves of NR and PHB as well as NR-g-PHB samples from -100 ^{o}C to 190 ^{o}C. The corresponding thermal data, including the glass transition temperature (T_g), melting temperature (T_m), crystallization temperature (T_c) and the calculated polymer's crystallinity (χ_c) are listed in Table 3. Generally, the DSC curve in Figure 15 (a) showed only a single T_g at 8.6 ^{o}C for PHB, while the T_m peak of the purified PHB occurred at 172.1 ^{o}C. Similar result was obtained in a previous report [28]. In contrast, the measured T_g of NR is -60.9 ^{o}C with the absence of T_m and T_c peaks.

A single and distinct T_g was observed in all NR-g-PHB samples. The T_g for 3, 5, 7 and 10 % mol of BPO were 0.6 ^{o}C, -1 ^{o}C, 2.9 ^{o}C and -0.5 ^{o}C respectively. Herein, the appearance of single a T_g indicated no phase separation and confirmed that grafting reaction occurred. In addition, the 7 % mol of BPO loadings showed a higher T_g probably due to the presence of the bulky grafted PHB on the NR molecule which caused restriction on the chain mobility.

Besides that, two T_m peaks were observed in all grafted samples as shown in Figure 15 (b). The T_m of all NR-g-PHB samples was slightly shifted to lower temperature as compared to pristine PHB. For example, the T_m peaks for PHB was 172 ^{o}C, while for NR-g-PHB prepared using 3, 5, 7 and 10 % mol, T_m values were 143-154 ^{o}C, 141.3-153.4 ^{o}C, 141.2-155.1 ^{o}C as well as 144.7-158.0 ^{o}C correspondingly. This occurrence may be due to the presence of ungrafted and shorter PHB chains in the NR-g-PHB. Furthermore, the double melting behavior might be explained by the dispersion of NR particles in PHB matrix that inhibited the crystallization of PHB, which lead to the formation of imperfect crystals. Meanwhile, Xu et al. [36] revealed the formation of the double T_m peaks was attributed to the melting of the crystals formed during the non-isothermal crystallization for the first T_m peak, whereas the second T_m peak corresponded to the melting of the crystals formed through recrystallization and reorganization of the crystals of the first T_m peak during the subsequent DSC heating scans.

Subsequently, pristine PHB has no crystallization peak temperature (T_c). However, in the case of NR-g-PHB prepared using 3, 5, 7 and 10 % mol, T_c occurs to around 77.3 ^{o}C, 87.5 ^{o}C, 90.3 ^{o}C and 85.9 ^{o}C respectively. It was obvious that T_c of the NR-g-PHB was always high, indicating that the presence of NR played a role in accelerating the crystallization of PHB due to the nucleation effect in the graft polymer. Similar phenomenon was reported elsewhere [36]. The

values for degree of crystallinity were lower after grafting in comparison with the PHB 55 %. This trend is due to the existence of amorphous NR which hindered the crystal structure of PHB [6]. This was in good agreement with the increased crystallization temperatures (T_c) of all grafted copolymers as compared to bulk PHB.

(a)

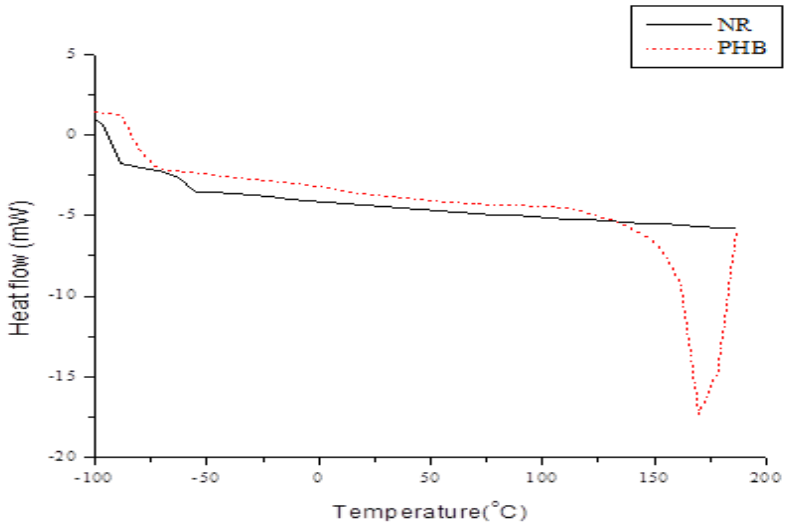

(b)

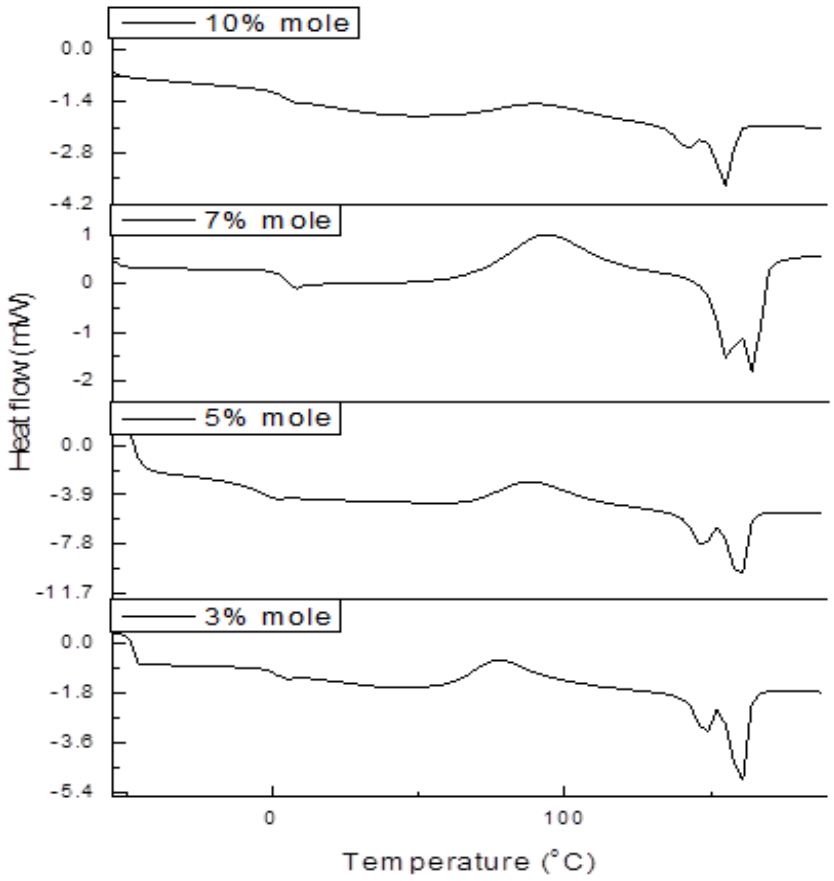

Figure 15: DSC thermogram for NR, PHB and NR-g-PHB using various initiators 3, 5, 7 and 10 % mol.

Table 3: Thermal transitions of NR, PHB and various NR-g-PHB.

BPO Loadings	2nd heating scan				
	T_{g1} (°C)	T_{m1} (°C)	T_{m2} (°C)	T_C (°C)	χ_c (%)
NR	-60.9	-	-	-	-
3	0.6	143.0	154.0	77.3	25.0
5	-1.0	141.3	153.4	87.5	32.0
7	2.9	141.2	155.1	90.3	39.7
10	-0.5	144.7	158.0	85.9	40.6
PHB	8.6	172.1	-	-	55.0

4.0 Conclusion

In summary, this work describes a grafting study of PHB onto NR. The use of BPO enabled PHB to be grafted onto NR in a simple process at relatively mild temperature for limiting PHB thermal degradation. The properties of the NR-g-PHB materials could be tuned by varying reaction conditions. Herein, 105 ^{o}C for reaction temperature with 7 % mol of BPO are the optimum conditions for grafting NR with PHB. The grafting sites between PHB and NR were analyzed using complementary NMR techniques and the reaction mechanism was confirmed by the appearance of new ^{1}H and ^{13}C NMR peaks. Besides that, DEPT 90 and 135 also showed consistent results with the proposed structure for the grafted copolymer. Additionally, FTIR show a consistent trend with NMR analyses. Meanwhile, a single glass transition temperature was observed from DSC, which indicated no phase separation occurred for the grafted samples. In addition, due to the new bonds formed via grafting the thermal stability of NR-g-PHB was improved as compared to pristine PHB and NR.

Acknowledgement

The authors would like to acknowledge (i) the financial support from research grant scheme (RU 1001/PKIMIA/8011071) and also ministry of higher education for scholarship.

5.0 References

[1] R.A.J. Verlinden, D.J. Hill, M.A. Kenward, C.D. Williams and I. Radecka, Bacterial Synthesis of biodegradable polyhydroxyalkanoates, Journal of Applied Microbiology, 102 (2007), 1437–1449.

[2] P. Ma, D. G. Hristova-Bogaerds, P. J. Lemstra, Y. Zhang, S. Wang, Toughening of PHBV/PBS and PHB/PBS blends via in situ compatibilization using dicumyl peroxide as a free-radical grafting initiator, Macromolecular Materials Engineering, 297 (2012), 402–410

[3] M. I. Artsis, A. P. Bonartsev, A. L. Iordanskii, G. A. Bonartseva, G. E. Zaikov, Biodegradation and medical application of microbial poly (3-Hydroxybutyrate), Molecular Crystallization Liquid Crystallization, 555 (2012), 232–262.

[4] I. Manavitehrani, A. Fathi, H. Badr, S. Daly, A. N. Shirazi and F. Dehghani, Biomedical applications of biodegradable polyesters, Polymers, 8 (2016), 1-32.

[5] Ana P. Heitmanna, Patrícia S.O. Patrício, Italo R. Coura, Emerson F. Pedroso, Patterson P.

Souza, Herman S. Mansur, Alexandra Mansur, Luiz C.A. Oliveira, Nanostructured Niobium Oxyhydroxide Dispersed Poly (3-hydroxybutyrate) (PHB) films: Highly Efficient Photocatalysts for Degradation Methylene Blue Dye, Applied Catalysis B: Environmental, 189 (2016), 141–150.

[6] L. Wei, A. G. McDonald, N. M. Stark, Grafting of Bacterial Polyhydroxybutyrate (PHB) onto Cellulose via In-Situ Reactive Extrusion with Dicumyl Peroxide, Biomacromolecules, Just Accepted Manuscript • DOI: 10.1021/acs.biomac.5b00049.

[7] A.A. Ol'khov, L.S. Shibryaeva, Y. V. Tertyshnaya, A.N. Kovaleva, E.L. Kucherenko, A.L. Zhul'kina, and A.L. Iordanskii, Resistance to Thermal Oxidation of Ethylene Propylene Rubber and Polyhydroxybutyrate Blends, International Polymer Science and Technology, 44 (2017), 6-10.

[8] M. Avella, M. E. Errico, B. I. M. Malinconico, L. F. L. Paolillo, Preparation of Poly(β-hydroxybutyrate)/Poly(methyl methacrylate) Blends by Reactive Blending and Their Characterization, Macromolecule Chemical Physic, 199 (1998), 1901-1907.

[9] H. J. Chiu, J. W. You, Lamellar Morphology of Poly (3-hydroxybutyrate)/Poly (ethylene oxide) Blends as Studied via Small Angle X-ray Scattering, Journal of Polymer Research, 10 (2003), 79–85.

[10] D. Lovera, L. Ma´rquez, V. Balsamo, A. Taddei, C. Castelli, A. J. Mu¨ller, Crystallization, Morphology, and Enzymatic Degradation of Polyhydroxybutyrate/Polycaprolactone (PHB/PCL) Blends, Macromolecule Chemical Physic, 208 (2007), 924–937.

[11] P. Greco, E. Martuscelli, Crystallization and Thermal Behaviour of poly(D-3-hyd roxybutyrate)-Based Blends, Polymer, 30 (1989), 1475-1483.

[12] J. T. Sakdapipanich, P. Rojrutha, Molecular Structure of Natural Rubber and Its Characteristics Based on Recent Evidence, 13 (2012)214-238.

[13] T. Jiang, P. Hu, Radiation Induced Graft Polymerization of Isoprene onto Polyhydroxybutyrate, Polymer Journal, 33 (2001), 647-653.

[14] C. Chen, S. Peng, B. Fei, Y. Zhuang, L. Dong, Z. Feng, S. Chen, H. Xia, Synthesis and Characterization of Maleated Poly(3-hydroxybutyrate), Journal of Applied Polymer Science, 88 (2003), 659 – 668.

[15] S. G. Hong, Y. C. Lin, C. H. Lin, Improvement of the Thermal Stability of Polyhydroxybutyrates by Grafting with Maleic Anhydride by Different Methods:

Differential Scanning Calorimetry, Thermogravimetric Analysis, and Gel Permeation Chromatography, Journal of Applied Polymer Science, 110 (2008), 2718–2726.

[16] P. Ma, X. Cai, X. Lou, W. Dong, M. Chen, P. J. Lemstra, Styrene-Assisted Melt Free-Radical Grafting of Maleic Anhydride onto Poly(b-hydroxybutyrate), Polymer Degradation and Stability, 100 (2014), 93-100.

[17] H. K. Lee, J. Ismail, H. W. Kammer, M. A. Bakar, Melt Reaction in Blends of Poly(3-hydroxybutyrate) (PHB) and Epoxidized Natural Rubber (ENR-50), Journal of Applied Polymer Science, 95 (2005), 113–129.

[18] B. N. Misra, R. Dogra, I. Kaur, D. Sood, Grafting onto Starch. II.Graft Copolymerization of Vinyl Acetate onto Starch by Radical Initiator, Journal Polymer Science: Polymer Chemistry Edition, 18 (1980), 341-344.

[19] S. Moolsin, N. Saksayamkul, A. N. Wichien, Natural Rubber Grafted Poly (methy methacrylate) as Compatibilizer in 50/50 Natural Rubber/Nitrile Rubber Blend, Journal of Elastomers and Plastics, 49 (2016), 422-439.

[20] K. Formela, M. Marc, S. Wang, M. R. Saeb, Interrelationship between Total Volatile Organic Compounds Emissions, Structure and Properties of Natural Rubber/ Polycaprolactone Bio-Blends Cross-linked with Peroxides, Polymer Testing, 60 (2017), 405-412.

[21] F. Dghima, M. Bouaziz, I. Mezghani, M. Boukhris, M. Neffati, Laticifers identification and Natural Rubber Characterization from The Latex of Periploca Angustifolia Labill. (*Apocynaceae*), Flora, 217 (2015), 90–98.

[22] S. Kawaharaa, O. Chaikumpollerta, S. Sakuraib, Y. Yamamotoa, K. Akabori, Crosslinking Junctions of Vulcanized Natural Rubber Analyzed by Solid-State NMR Spectroscopy Equipped with Field-Gradient-Magic Angle Spinning Probe, Polymer, 50 (2009), 1626-1631.

[23] P. C. D. Oliveira, A. M. D. Oliveira, A. Garcia, J. C. D. Souza Barboza, C. A. D. Carvalho Zavaglia, A. M. D. Santos, Modification of Natural Rubber: A Study by ^{1}H NMR to Assess The Degree of Graftization of Poly-DMAEMA or Poly-MMA onto Rubber Particles Under Latex Form in The Presence of a Redox Couple Initiator, European Polymer Journal, 41 (2005), 1883–1892.

[24] T. Saito, W. Klinklai, S. Kawahara, Characterization of Epoxidized Natural Rubber by 2D

NMR Spectroscopy, Polymer, 48 (2007), 750-757.

[25] S. Kawahara, J. Ukawa, J. Sakai, Y. Yamamoto, Y. Isono, High- Resolution Latex-State ^{13}C-NMR spectroscopy for natural rubber vulcanizates, Rubber Chemistry And Technology, 80 (2007), 751-761.

[26] N. Choothong, K. Kosugi, Y. Yamamoto, S. Kawahara, Characterization of Brominated Natural Rubber by Solution-state 2D NMR Spectroscopy, Reactive and functional Polymers, 113 (2017) 6-12.

[27] M. A. Hassan, E. K. Bakhiet, S. G. Ali, H. R. Hussien, Production and Characterization of Polyhydroxybutyrate (PHB) Produced by *Bacillus sp.* Isolated from Egypt, Journal of Applied Pharmaceutical Science, 6 (2016), 46-51.

[28] V. U. Irorere, S. Bagherias, M. Blevins, I. Kwiecie, A. Stamboulis, I. Radecka, Electrospun Fibres of Polyhydroxybutyrate Synthesized by *Ralstonia eutropha* from Different Carbon Sources, International Journal of Polymer Science, 8 (2014), 1-11.

[29] A. Brinda Devi, C. Valli Nachiyar, T. Kaviyarasi, Antony V. Samrot, Characterization of Polyhydroxybutyrate Synthesized by *Bacillus Cereus*, International Journal Pharmaceutical Science, 7 (2015) 140-144.

[30] W.L.Tan, N.N. Yaakob, A. Zainal Abidin, M. Abu Bakar and N.H.H. Abu Bakar, Metal Chloride Induced Formation of Porous Polyhydroxybutyrate (PHB) Films: Morphology, Thermal Properties and Crystallinity, IOP Conf. Series: Materials Science and Engineering, 133 (2016), 1-12.

[31] J. A. López, J. M. Naranjo, J. C. Higuita, M. A. Cubitto, C. A. Cardona, M. A. Villar, Biosynthesis of PHB from a New Isolated *Bacillus Megaterium* Strain: Outlook on Future Developments with Endospore Forming Bacteria, Biotechnology and Bioprocess Engineering, 17 (2012), 250-258.

[32] Y. Doi, M. Kunioka, Y. Nakamura, K. Soga, Proton and Carbon NMR Analysis of Poly(β-hydroxybutyrate) Isolated from *Bacillus Megaterium*, Macromolecules, 19 (1986), 1271-1276.

[33] C. R. Arza, P. Jannasch, P. Johansson, P. Magnusson, A. Werker, F. H. J. Maurer, Effect of Additives on The Melt Rheology and Thermal Degradation of Poly[(R)-3-Hydroxybutyric acid], Journal of Applied Polymer Science, 132 (2015), 1-6.

[34] E. Bugnicourt, P. Cinelli, A. Lazzeri, V. Alvarez, Polyhydroxyalkanoate (PHA): Review of

Synthesis, Characteristics, Processing and Potential Applications in Packaging, eXPRESS Polymer Letters, 8 (2014), 791–808.

[35] S. Rolere, S. Liengprayoon, L. Vaysse , J. Sainte-Beuve, F. Bonfils, Investigating Natural Rubber Composition with Fourier Transform Infrared (FT-IR) Spectroscopy: A Rapid and Non-Destructive Method to Determine Both Protein and Lipid Contents Simultaneously, Polymer Testing, 43 (2015), 83-93.

[36] C. Xu, Z. Qiu, Non-isothermal Melt Crystallization and Subsequent Melting Behavior of Biodegradable Poly (hydroxybutyrate)/ Multiwalled Carbon Nanotubes Nanocomposites, Journal of Polymer Science: Part B: Polymer Physics, 47(2009), 2238–2246.